Carcinogenesis vol.30 no.3 pp.512–519, 2009
doi:10.1093/carcin/bgp015
Advance Access publication January 9, 2009

Phosphoaspirin (MDC-43), a novel benzyl ester of aspirin, inhibits the growth of human cancer cell lines more potently than aspirin: a redox-dependent effect

Wenping Zhao, Gerardo G.Mackenzie, Onika T.Murray, Zhiquan Zhang and Basil Rigas*

Department of Medicine, Division of Cancer Prevention, Life Sciences Building, Room 06, Stony Brook University, Stony Brook, NY 11794-5200, USA

*To whom correspondence should be addressed. Tel: +1 631 632 9035; Fax: +1 631 632 1992;
Email: basil.rigas@stonybrook.edu

Aspirin is chemopreventive against colon and probably other cancers, but this effect is relatively weak and its chronic administration to humans is associated with significant side effects. Because of these limitations, extensive effort has been exerted to improve the pharmacological properties of aspirin. We have determined the anticancer activity and mechanisms of action of the novel *para* positional isomer of phosphoaspirin [P-ASA; MDC-43; 4-((diethoxyphosphoryloxy)methyl)phenyl 2-acetoxybenzoate]. P-ASA inhibited the growth of 10 human cancer cell lines originating from colon, lung, liver, pancreas and breast, at least 18- to 144-fold more potently than conventional aspirin. P-ASA achieved this effect by modulating cell kinetics; compared with controls, P-ASA reduced cell proliferation by up to 68%, increased apoptosis 5.5-fold and blocked cell cycle progression in the G_2/M phase. P-ASA increased intracellular levels of reactive oxygen species (ROS), depleted glutathione levels and modulated cell signaling predominantly through the mitogen-activated protein kinase (p38 and c-jun N-terminal kinase), cyclooxygenase (COX) and nuclear factor-kappa B pathways. P-ASA targeted the mitochondria, increasing mitochondrial superoxide anion levels; this effect on ROS led to collapsed mitochondrial membrane potential and triggered the intrinsic apoptotic pathway. The antioxidant *N*-acetyl cysteine abrogated the cell growth inhibitory and signaling effects of P-ASA, underscoring the centrality of ROS in its mechanism of action. Our results, establishing P-ASA as a potent inhibitor of the growth of several human cancer cell lines, suggest that it may possess broad anticancer properties. We conclude that the novel P-ASA is a promising anticancer agent, which merits further evaluation.

Introduction

The discovery that nonsteroidal antiinflammatory drugs (NSAIDs) are effective chemopreventive agents against a variety of human cancers represents a major breakthrough in the field of cancer prevention. Based on extensive epidemiological data assessing NSAID use in preventing major human cancers, aspirin appears to be one of the most effective NSAIDs in cancer prevention (1). Although aspirin has formally been proven to be chemopreventive against human colon cancer (2), its effect is relatively weak and its chronic administration, as would be required for its use in chemoprevention, is associated with significant side effects (3). Because of these limitations, extensive effort has been exerted to improve the pharmacological properties of aspirin (4,5).

Abbreviations: BSO, D,L-buthionine (*S*,*R*)-sulfoximine; COX, cyclooxygenase; DAF-FM, 4-amino-5-methylamino-2′,7′-difluorofluorescein; DCFDA, 2′,7′-dichlorodihydrofluorecein diacetate; DHE, dihydroethidium; ERK, extracellular signal-regulated kinase; GSH, glutathione; IC_{50}, 50% inhibitory concentration; JC-1, 5,5′,6,6′-tetrachloro-1,1′,3,3′-tetraethylbenzimidazolylcarbocyanine iodide; JNK, c-jun N-terminal kinase; MAPK, mitogen-activated protein kinase; NAC, N-acetyl-L-cysteine; NF-κB, nuclear factor-kappa B; P-ASA, phosphoaspirin; PI, propidium iodide; ROS, reactive oxygen species.

Ongoing work in our laboratory evaluates a series of novel acyloxy benzyl esters, which have anticancer properties. We have recently reported our findings concerning a novel acyloxy benzyl ester-based derivative of aspirin (MDC-63; the *meta* positional isomer in Figure 1), which showed two potentially significant features: (i) efficacy in a murine model of cancer, achieving >60% reduction in tumor volume of xenografted HT-29 human cancer cells, and (ii) no apparent toxicity, evidenced, among others, by the absence of changes in body weight during treatment and organ damage (6). The mode of action of this compound includes, at the cytokinetic level, brisk induction of apoptosis and some suppression of proliferation.

As can be appreciated from Figure 1, this molecule lends itself to positional isomerism. The diethylphosphate group can occupy any of three positions on the benzene ring, *o*-, *m*- or *p*- with respect to the ester bond between aspirin and its linker molecule. Since positional isomerism can at times have a profound effect on the pharmacological properties of a drug (7), we decided to evaluate the effect of the *para* isomer (MDC-43) on the growth of various human cancer cell lines; to study its mechanism of action, we subsequently focused on SW480 human colon cancer cells.

We observed that the growth inhibitory effect of *p*-phosphoaspirin (P-ASA; MDC-43), independent of the tissue origin of the cancer cell lines, was mediated by elevated intracellular levels of reactive oxygen species (ROS), which in turn activated relevant cell signaling. Our results suggest the anticancer potential of P-ASA and indicate that this class of compounds merits further evaluation.

Materials and methods

Reagents

p-Phosphoaspirin (MDC-43) was a gift of Chem-Master International, East Setauket, NY. Dihydroethidium (DHE), 2′,7′-dichlorodihydrofluorecein diacetate (DCFDA), 4-amino-5-methylamino-2′,7′-difluorofluorescein (DAF-FM), MitoTracker Green FM, MitoSOX Red and Annexin V were purchased from Invitrogen (Carlsbad, CA). Conventional aspirin and *N*-acetyl-L-cysteine (NAC) were purchased from Sigma (St Louis, MO).

Cell culture and cell kinetic assays

Human colon (HT-29, LoVo, HCT116, HCT-15 and SW480), pancreatic (BxPC-3 and MIA PaCa-2), breast (MCF-7), liver (Hep G2) and lung (H838) cell lines (American Type Culture Collection, Manassas, VA) were grown in media as per the instructions of American Type Culture Collection. The cell viability/growth response to P-ASA was measured using the 3-(4, 5-dimethylthiazol-2-yl)-2, 5-diphenyl tetrazolium bromide assay (Roche Diagnostics Indinapolis, IN) or the trypan blue exclusion method.

To measure cell proliferation (i.e. cell renewal), SW480 cells, treated with P-ASA for 24 h, were pulse labeled with 10 μM bromodeoxyuridine BD Bioscience (San Jose, CA) 15 min prior to harvesting and analyzed by flow cytometry. To measure apoptosis and necrosis, SW480 cells were treated with P-ASA for 18 h, harvested by trypsinization, stained with fluorescein isothiocyanate-conjugated Annexin V and propidium iodide (PI) as per the manufacturer's protocol and subjected to flow cytometry analysis. For cell cycle analysis, cells were stained with PI following standard protocols.

Detection of ROS

SW480 cells were pretreated with ROS probes (5 μM DCFDA, 5 μM DHE, 2 μM DAF-FM or 5 μM MitoSOX Red) in RPMI 1640 medium without fetal bovine serum or phenol red for 1 h (30 min in the case of MitoSOX Red). This was followed by treatment with 25 μM P-ASA for 1 h. Finally, cells were washed and analyzed by flow cytometry. For ROS live imaging, SW480 cells were pretreated with 5 μM MitoSOX Red for 30 min followed by MitoTracker Green FM for 10 min. The cells were then treated with 25 μM P-ASA for 1 h. Images were captured with a Zeiss LSM510 meta confocal microscope and processed in Adobe Photoshop.

Determination of glutathione levels

The levels of glutathione (GSH) were determined by the GSH reductase-coupled 5,5′-dithiobis-(2-nitrobenzoic acid) assay, based on the 5,5′-dithiobis-(2-nitrobenzoic acid)/enzymatic recycling procedure of Tietze (8). Briefly,

50 µl of each working standard or diluted sample extract was added to the wells of a flat-bottomed 96-well microtiter plate. All standards and samples were run in duplicate in adjacent wells. Fifty microliters of 5,5′-dithiobis-(2-nitrobenzoic acid) 1.26 mM and 50 µl of GSH oxidoreductase 2.5 kU/l were then added to each well and after 15 min at room temperature, the reaction was started by the addition of 50 µl of 0.72 mmol/l of reduced nicotinamide adenine dinucleotide phosphate to each well. Absorbance was measured at 410 nm using a 96-well plate reader (SpectraMax M5, Molecular Devices, Sunnyvale, CA). Data were analyzed using SoftMax Pro v5 software.

Determination of mitochondrial membrane potential

The mitochondrial membrane potential was determined by flow cytometry using the 5,5′,6,6′-tetrachloro-1,1′,3,3′-tetraethylbenzimidazolylcarbocyanine iodide (JC-1) cationic dye (Invitrogen). In healthy cells, the JC-1 dye stains the mitochondria bright red, but in apoptotic cells, in which the mitochondrial membrane potential collapses, it remains in the cytoplasm in its green fluorescence form. Briefly, SW480 cells were incubated with 1.5× 50% Inhibitory Concentration (IC_{50}) P-ASA for 3 h, when cells were trypsinized and washed once with phosphate-buffered saline. The supernatant was discarded and cells were incubated with 5 µM JC-1 for 30 min at 37°C protected from light and analyzed by flow cytometry using the FL1 and FL2 (green and red fluorescence, respectively).

Western blot

Cell lysates (20 µg of total protein) were resolved in 10% sodium dodecyl sulfate–polyacrylamide gel and transferred onto polyvinylidene fluoride membranes. Membranes were probed with antibodies against p38, p-p38, c-jun N-terminal kinase (JNK), p-JNK, extracellular signal-regulated kinase (ERK), p-ERK, AKT, p-AKT and caspase 9 Cell Signaling (Beverly, MA), procaspase 8 Santa Cruz (Santa Cruz, CA) or cyclooxygenase (COX)-2 Cayman Chemical (Ann Arbor, MI). β-Actin (Sigma) was used as the loading control.

Electrophoretic mobility shift assay

After the indicated treatment of cells, nuclear fractions were isolated from 3×10^6 cells, as described previously (9,10). The oligonucleotide containing the consensus sequence for nuclear factor-kappa B (NF-κB) was end labeled with [γ-^{32}P]adenosine triphosphate using T4 polynucleotide kinase. Samples were incubated with the labeled oligonucleotide (20 000–30 000 c.p.m.) for 20 min at room temperature in binding buffer [10 mM Tris–HCl buffer, pH 7.5, containing 4% (vol/vol) glycerol, 1 mM $MgCl_2$, 0.5 mM ethylenediaminetetraacetic acid, 0.5 mM dithiothreitol, 50 mM NaCl and 0.05 mg/ml poly(dI-dC)]. The reaction products were separated by electrophoresis in a 6% (wt/vol) nondenaturing polyacrylamide gel using 0.5× TBE (45 mM Tris–borate and 1 mM ethylenediaminetetraacetic acid, pH 8.3) as the running buffer. The gels were dried and the radioactivity was quantified.

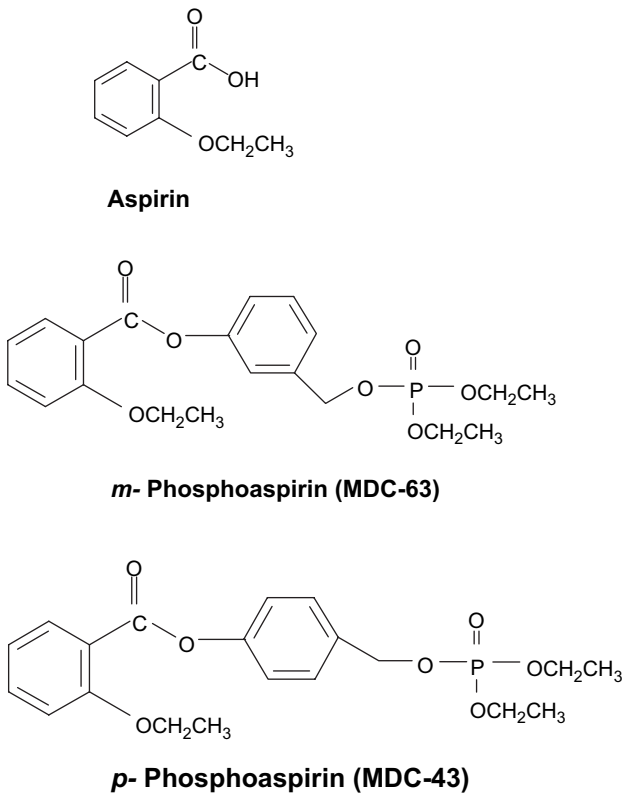

Fig. 1. Chemical structures of aspirin, *m*-phosphoaspirin (MDC-63) and *p*-phosphoaspirin (MDC-43). An aromatic linker molecule binds diethylphosphate to the carboxyl group of conventional aspirin. The position of diethylphosphate on the benzene ring of the linker moiety defines the two isomers.

Enzyme-linked immunosorbent assay

Trypsinized cells were suspended in lysis buffer to which Nonidet P-40 was added in a subsequent step; nuclei were washed and centrifuged, followed by resuspension in extraction buffer and centrifuged. Nuclear extracts were stored at −80°C until assayed. TransBinding NF-κB assay was performed using an ELISA kit (Panomics, Fremont, CA) and following the manufacturer's protocol.

Statistical analysis

Statistical evaluation of the data was performed by one-factor analysis of variance followed by Tukey's test for multiple comparisons. $P < 0.05$ was regarded statistically significant. The data, obtained from at least three independent experiments, were expressed as the mean ± SEM.

Results

P-ASA inhibits the growth of various human cancer cell lines

We evaluated the growth inhibitory effect of P-ASA on human cancer cell lines originating from the colon, pancreas, breast, lung and liver. Cells plated at a density of $5.5 \times 10^4/cm^2$ were treated with P-ASA for 24 h and their IC_{50} was determined.

As shown in Table I, the most sensitive cell line was HepG2 (IC_{50} = 13.8 µM), whereas the least sensitive was the pancreatic cell line MIA PaCa-2 (IC_{50} = 113 µM), being ∼8-fold higher than that of HepG2. In general, the IC_{50} values of these cell lines do not differ greatly among themselves and in the case of the five colon cancer cell lines, their range of values is even narrower (14.3–67.6 µM).

In agreement with previous findings (11), conventional ASA in concentrations up to 2 mM failed to inhibit the growth of any of these cell lines by 50% or more; thus, its IC_{50} values could not be determined. In all 10 cell lines that we studied, P-ASA was more potent than aspirin; the fold enhancement of potency ranged between >18 and >144, being on average >66.8. Of note, *para* P-ASA is more potent than its *meta* isomer [(6) and similar data not shown].

Cell kinetic effect of P-ASA on SW480 human colon cancer cells

To explore the mechanism of the growth inhibitory effect of P-ASA, we determined its effect on cell renewal, cell death and cell cycle (Figure 2).

Table I. P-ASA (MDC-43) inhibits the growth of human cancer cell lines

Cell lines	IC_{50} (µM) (mean ± SD)		
	P-ASA	Aspirin	Aspirin/P-ASA
Colon			
HT-29	42.6 ± 10.6	>2000	>46
HCT-15	14.3 ± 6.7	>2000	>140
SW480	23.1 ± 3.9	>2000	>86
Lovo	46.6 ± 7.3	>2000	>42
HCT116	67.6 ± 10.4	>2000	>29
Pancreas			
BxPC3	27.4 ± 6.3	>2000	>72
MIA PaCa-2	113 ± 17.8	>2000	>18
Liver			
HepG2	13.8 ± 5.8	>2000	>144
Lung			
H838	54.0 ± 4.5	>2000	>37
Breast			
MCF-7	38.0 ± 5.1	>2000	>52

SW480 cells were incubated overnight and then treated with P-ASA as indicated. Cell renewal (proliferation) was evaluated by the bromodeoxyuridine method. P-ASA reduced bromodeoxyuridine incorporation concentration-dependently, decreasing it by 68% at 50 μM, the highest concentration used. After 24 h of incubation, there was cell cycle arrest in G_2/M phase, evident at all drug concentrations. Treatment with 25 μM P-ASA for 18 h increased the proportion of apoptotic cells 5.5-fold compared with controls. The greatest increase, 8.4-fold over control, was in late apoptotic cells [Annexin V (+)/PI(+)]; early apoptotic cells [Annexin V (+)/PI(−)] were increased only 3.1-fold. Finally, P-ASA increased 4-fold the number of purely necrotic cells [Annexin V (−)/PI(+)]. As detailed below, the antioxidant agent NAC prevented the growth inhibitory effect of P-ASA (Figure 2E).

P-ASA induces the production of ROS in SW480 cells

Previous work indicates that the induction of ROS by chemopreventive and chemotherapeutic agents represents a critical early event in their mechanism of action (12). Thus, we explored whether P-ASA induces the production of ROS. To this end, we used the following molecular probes: DCFDA, which reacts with nearly 10 individual species and is considered a 'general probe' for RONS (13); DHE, which detects intracellular superoxide anions; MitoSOX Red, which specifically detects mitochondrial superoxide anions and DAF-FM, which detects nitric oxide. SW480 cells were cultured and treated with P-ASA 25 μM for 1 h and the levels of ROS were determined.

As shown in Figure 3, P-ASA increased DCFDA and MitoSOX Red fluorescence, but not that of DHE and DAF-FM. Compared with controls, the ROS levels detected by DCFDA were increased by 33%. NO and cellular superoxide anion levels (detected by DHE) were not altered by P-ASA. In sharp contrast, superoxide anion levels specifically in the mitochondria were markedly elevated in response to P-ASA. As the image overlay of the mitochondrial probes MitoTracker Green FM and MitoSOX Red confirms, P-ASA 25 μM increased mitochondrial superoxide anion levels by 112%, compared with control.

To further assess the reliability of our detection, we employed the antioxidant NAC, a precursor of intracellular GSH (14,15). Pretreatment of SW480 cells with NAC 20 mM for 4 h reversed most of the induction of superoxide anion in the mitochondria, as detected by MitoSOX Red. Moreover, NAC reversed P-ASA-induced apoptosis and necrosis (Figure 2D) and also abrogated the inhibitory effect of P-ASA on cell number (Figure 2E).

P-ASA decreases thiol levels and induces intrinsic apoptosis: redox dependence

We determined the effect of P-ASA on the intracellular levels of GSH, one of the most important antioxidant systems in mammalian cells

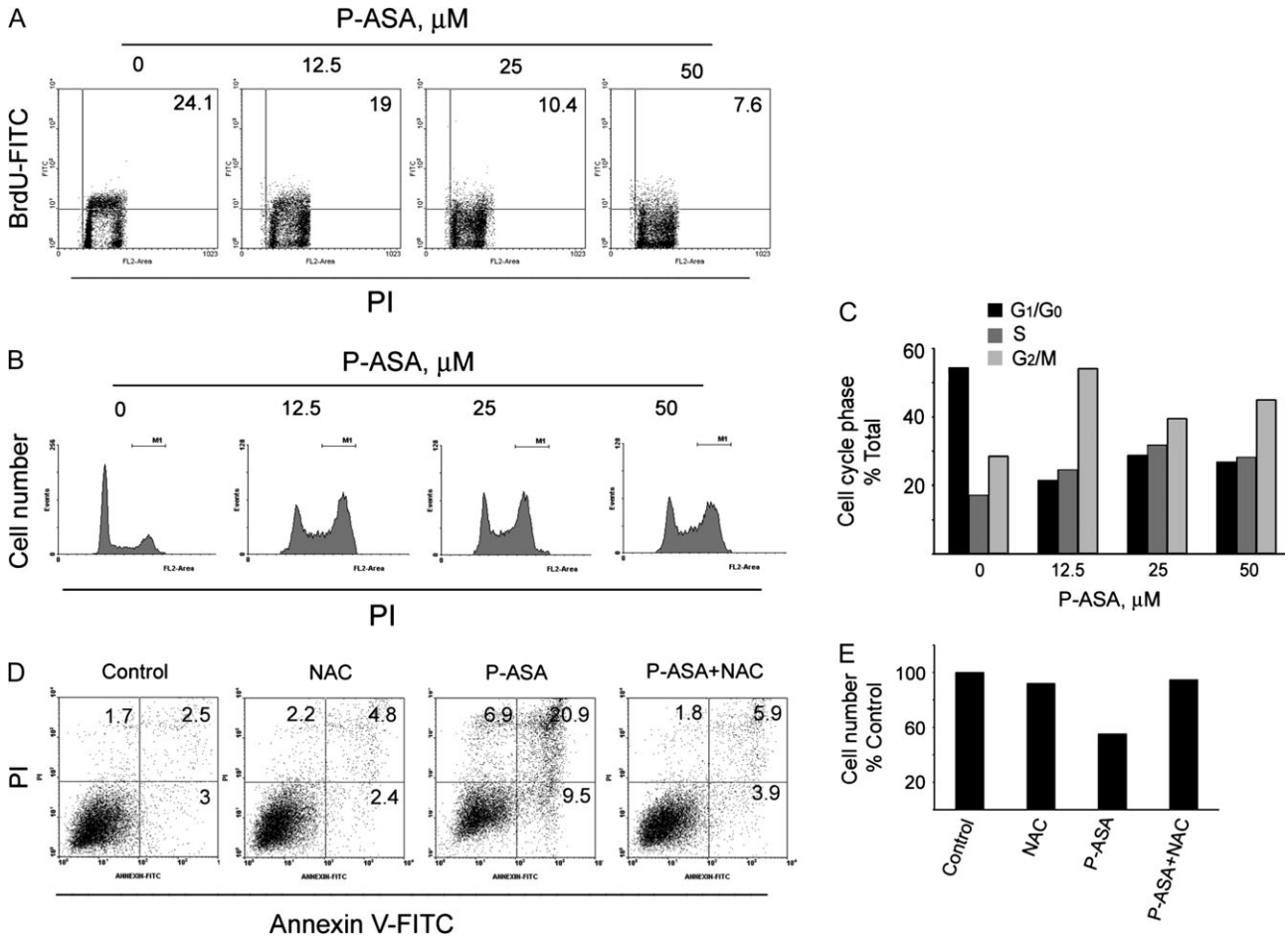

Fig. 2. The cell kinetic effect of P-ASA on SW480 colon cancer cells. SW480 cells were grown overnight and treated with P-ASA (MDC-43) as shown. (**A**) Cell proliferation assay based on bromodeoxyuridine (BrdU) incorporation into DNA during the S-phase of the cell cycle. The percentage of bromodeoxyuridine positive cells is shown in the right upper corner of each panel. (**B**) Cell cycle analysis by PI staining for DNA content of cells treated with and without P-ASA. Results, quantified in (**C**), demonstrate the induction of a G_2/M to G_0/G_1 block by P-ASA. (**D**) Flow cytometric analysis of cells stained with PI and Annexin V (A). A(−)/PI(−) cells are viable cells; A(+)/PI(−) are early apoptotic; A(+)/PI(+) are late apoptotic and A(−)/PI(+) are necrotic. The numbers inside each panel represent the percentage of cells in each category. NAC 20 mM was used to pretreat the cells for 4 h. (**E**) The effect of pretreatment with NAC on cell viability in response to P-ASA was determined by trypan blue staining and cell counting. Figures are representative of two experiments, whose results were within 10%.

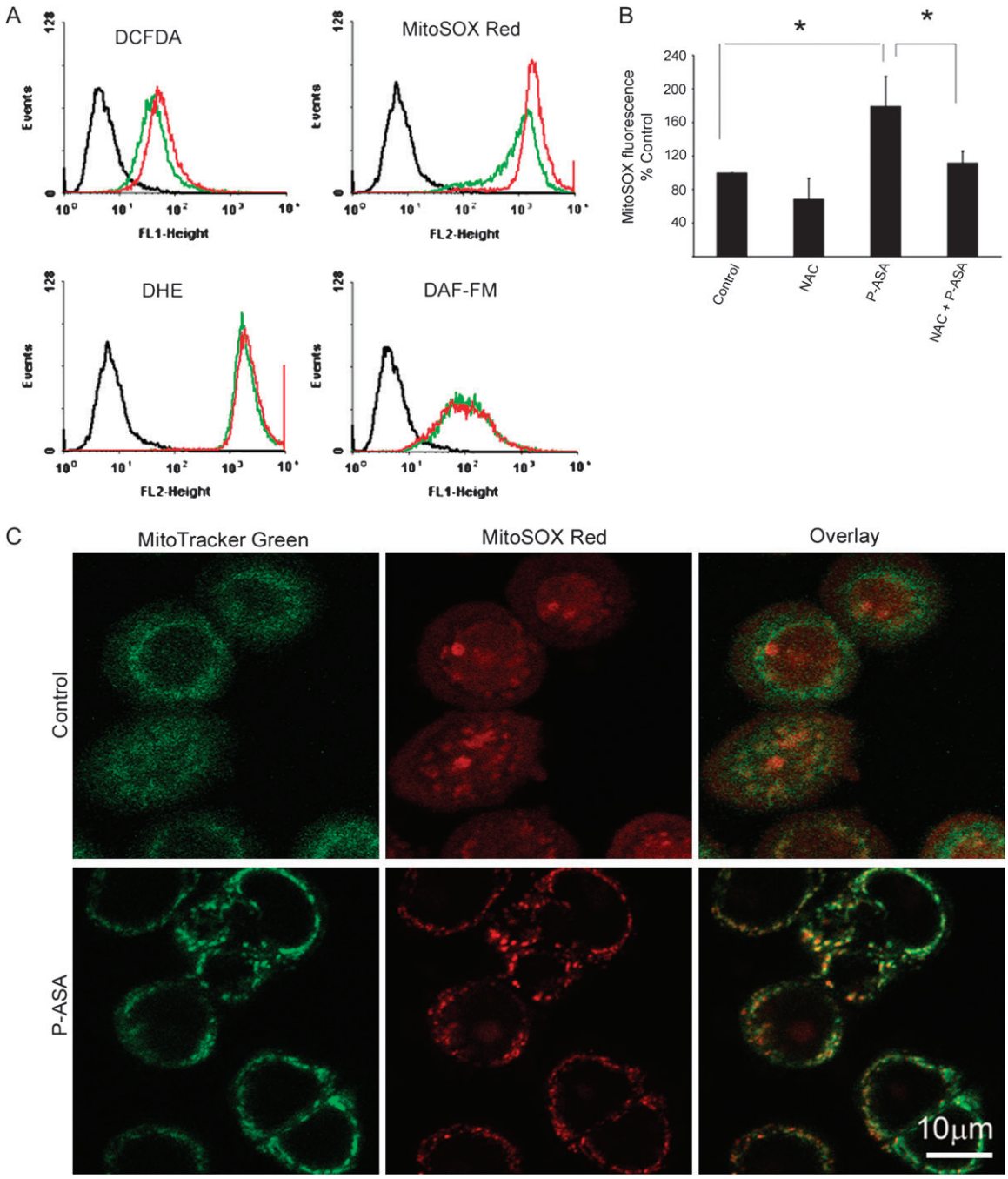

Fig. 3. The effect of P-ASA on ROS levels in SW480 colon cancer cells. (**A**) SW480 cells were preloaded with a molecular probe for ROS as indicated and treated with P-ASA (MDC-43) for 1 h. DCFDA is a general ROS probe; DHE detects superoxide anion in cells; MitoSOX Red detects specifically mitochondrial superoxide anion and DAF-FM detects NO. (**B**) Superoxide anion levels in mitochondria detected by MitoSOX Red were decreased following pretreatment with NAC. Values are the mean ± SEM of four independent experiments; $^{*}P < 0.05$. (**C**) Cells were stained with MitoSOX Red and MitoTracker Green, a stain specific for mitochondria. The overlay images (lower row) establish the mitochondrial origin of the increased superoxide anion levels in response to P-ASA.

(14). As shown in Figure 4, treatment of SW480 cells with P-ASA led to a significant concentration-dependent decrease of GSH levels. Incubation of SW480 cells with 80 μM P-ASA for 4 h decreased GSH levels by 35%. The GSH synthase inhibitor D,L-buthionine (*S*,*R*)-sulfoximine (BSO) (16) decreased GSH levels by 80%, whereas pretreatment with NAC 20 mM for 4 h largely restored GSH levels.

GSH depletion, induced by BSO, enhanced the cell growth inhibitory effect of P-ASA (Figure 4C). P-ASA 80 μM inhibited the growth of SW480 cells (IC_{50} 23 μM under our experimental protocol), but pretreatment with 10 μM BSO for 24 h reduced the IC_{50} to 11 μM. These findings clearly indicate that ROS controls the growth of cancer cells in response to P-ASA.

The two major pathways of apoptosis are the intrinsic, characterized by cytochrome *c* release and caspase 9 activation, and the extrinsic, involving activation of caspase 8 (17). To determine which pathway is operative in response to P-ASA, we assayed the levels of caspase 9 and 8 (Figure 4D). As indicated by the cleavage of procaspase 9, caspase 9 became activated. In contrast, no procaspase 8 cleavage was observed, indicating that the extrinsic pathway was not activated by P-ASA.

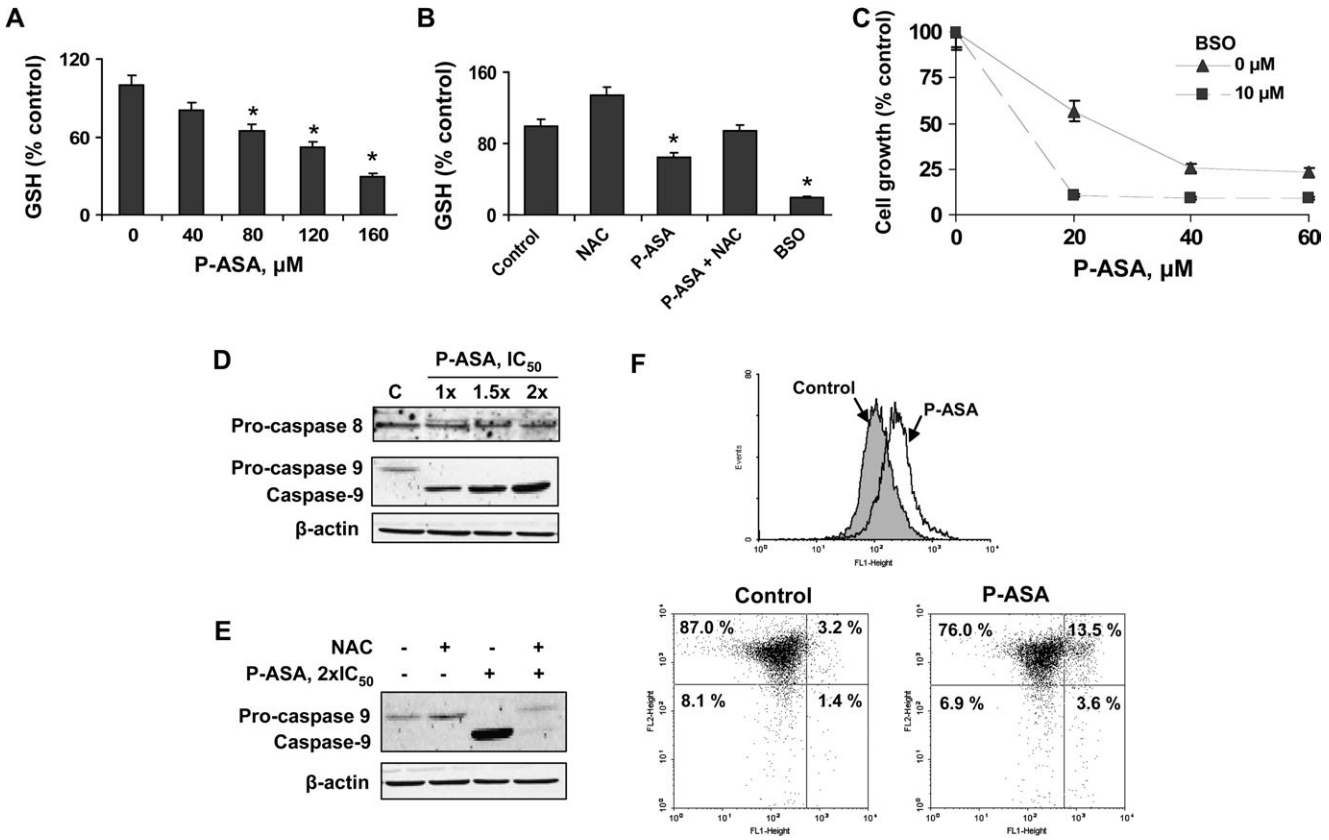

Fig. 4. P-ASA decreases thiol levels and induces intrinsic apoptosis in SW480 colon cancer cells. (**A**) SW480 cells were grown overnight and treated with various concentrations of P-ASA (MDC-43) for 4 h. GSH levels, determined as in Materials and Methods, were decreased in a concentration-dependent manner. Values are the mean ± SEM of three independent experiments. $^{*}P < 0.05$ compared with control. (**B**) Overnight pretreatment with 20 mM NAC restores GSH levels in P-ASA-treated cells. BSO, an inhibitor of GSH synthase, was used as a control for GSH depletion. (**C**) SW480 cells were treated with or without BSO for 24 h, followed by treatment with P-ASA for 18 h. Data (mean ± SEM of three experiments) are expressed as percent of control. (**D**) Inmunoblots for procaspase 8, procaspase 9 and caspase 9 in SW480 cells treated for 18 h with 1×, 1.5× or 2× IC_{50} P-ASA. Loading control: β-actin. (**E**) SW480 cells treated with P-ASA for 18 h following pretreatment with 20 mM NAC or vehicle for 4 h. Procaspase 9, caspase 9 and β-actin were detected by immunoblot. (**F**) SW480 cells were treated with P-ASA 1.5× IC_{50} for 3 h and their mitochondria membrane potential was determined by flow cytometry as described in Materials and Methods. Upper panel: fluorescence histograms of control SW480 cells and cells treated with P-ASA; the latter show a shift to the right indicating increased green fluorescence and thus collapsed mitochondrial membrane potential [the corresponding geometric means are as follows: control = 152 ± 17, P-ASA = 258 ± 27 (mean ± SEM)]. Lower panel: flow cytometry of SW480 cells stained as in Materials and Methods for mitochondrial membrane potential. Abscissa, FL1 (green fluorescence); ordinate, FL2 (red fluorescence). The shift toward green fluorescence indicates collapsed mitochondrial membrane potential.

To evaluate whether the altered redox state of the cell plays a role in the activation of caspase 9, we pretreated SW480 cells with NAC (18). NAC almost completely blocked the cleavage of caspase 9 induced by P-ASA at its IC_{50} concentration (Figure 4E). Since the mitochondria were involved in triggering cell death induced by P-ASA, we evaluated the effect of P-ASA on the mitochondrial membrane potential by using the JC-1 cationic dye. As shown in Figure 4F, incubation of SW480 cells with P-ASA 1.5× IC_{50} for 3 h increased green fluorescence by 70% compared with controls, indicating the collapse of the mitochondrial membrane potential. As seen in the lower panel of Figure 4F, the percentage of cells that display green fluorescence (right half of each panel) increased from 4.6% in controls to 17.1% in P-ASA-treated cells, i.e. it increased 3.7-fold.

Cell signaling effects of P-ASA in SW480 cells

To explore the effect of P-ASA on intracellular signaling pathways, we analyzed in cells treated with P-ASA the status of mitogen-activated protein kinases (MAPKs), ERK1/2, AKT, COX-2 and NF-κB.

As shown in Figure 5, P-ASA increased progressively in a time-dependent manner the levels of phosphorylated (i.e. activated) p38. This activation started 15 min after treatment with P-ASA and reached its highest level at 24 h, the last time point of observation. However, over the same period of time the levels of p38 remained unchanged, indicating an effect limited only to protein activation. JNK was similarly activated by phosphorylation, but this was an effect limited to a 7 h period, between 1 and 8 h post-treatment with P-ASA; at 24 h, the levels of p-JNK were barely detectable. Similar to p38, no change in the protein levels of JNK was noted, indicating again an effect limited to the activation of a signaling protein. We also noted modest changes in the levels of phosphorylated ERK1/2 (mainly at 3 h) and AKT (mainly between 1 and 8 h); the protein levels of both remained unchanged in response to P-ASA treatment. As shown in Figure 5C, NAC abrogated the activation of p38, JNK and ERK brought about by P-ASA, indicating its redox dependence.

COX-2 is a ROS-dependent enzyme (19). To investigate the effect of P-ASA on COX-2 signaling, we used the HT-29 colon cancer cell line because SW480 cells do not express COX-2. As shown in Figure 5D, P-ASA stimulated the expression of COX-2 in HT-29 cells in a concentration-dependent manner. The redox dependence of this effect was confirmed by its attenuation by pretreating these cells with 20 mM NAC.

Finally, we studied the effect of P-ASA on NF-κB activation. Both the enzyme-linked immunosorbent assay method and electrophoretic mobility shift assay gave concordant results, demonstrating that P-ASA suppressed NF-κB activity by >50% (Figure 5E and F). Again, as shown by the electrophoretic mobility shift assay study,

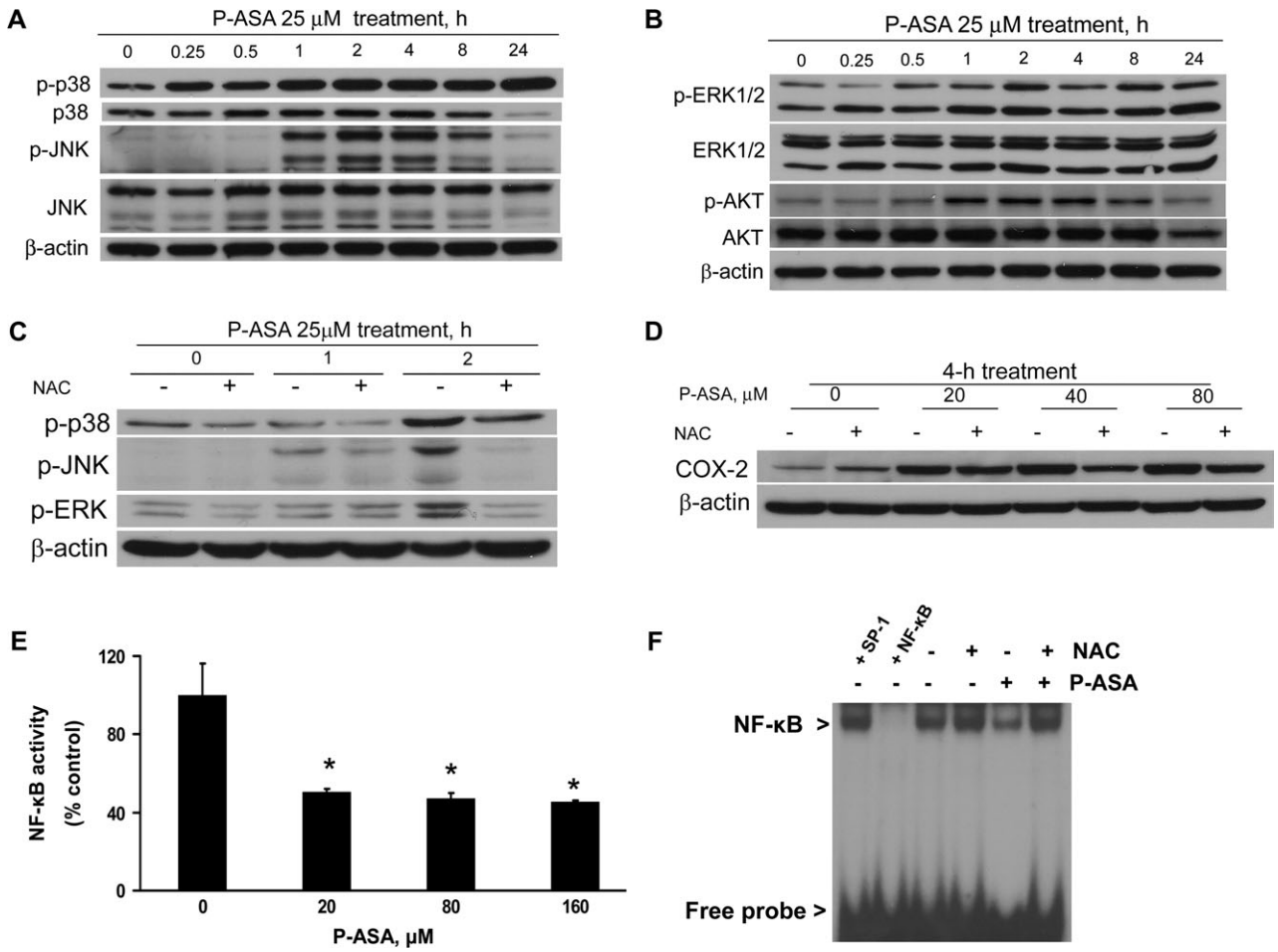

Fig. 5. Cell signaling effects of P-ASA in SW480 colon cancer cells. (**A** and **B**) SW480 cells were grown overnight and treated with 25 μM P-ASA (MDC-43) for up to 24 h, and the proteins shown were detected by immunoblot in whole-cell extracts. Phosphorylated (p-) and total p38, JNK, ERK and AKT were assayed. Loading control in A–D: β-actin. (**C** and **D**) Pretreatment with NAC 20 mM for 4 h reduces the activation of MAPKs and the induction of COX-2 in response to P-ASA treatment. (**E**) NF-κB-DNA binding was detected by an enzyme-linked immunosorbent assay method in SW480 cells treated with several concentrations of P-ASA for 4 h. Values are the mean ± SEM of three independent experiments; $^{*}P < 0.01$ compared with control. (**F**) Electrophoretic mobility shift assay for NF-κB in SW480 cells treated with 20 μM P-ASA for 4 h. NAC 20 mM was used to pretreat the cells for 4 h. To determine the specificity of the NF-κB-DNA complex, the control nuclear fraction was incubated before the binding assay with 100-fold molar excess of unlabeled oligonucleotide containing the sequence for NF-κB (lane labeled +NF-κB) or an unrelated transcription factor (lane labeled +SP-1).

pretreatment with 20 mM NAC restored NF-κB binding to its cognate DNA sequence, in agreement with the well-known redox sensitivity of NF-κB (20).

Discussion

Our data establish the strong growth inhibitory effect of P-ASA on human cancer cells. This effect (i) far exceeds that of aspirin, its parent molecule; (ii) appears to be generalized, and (iii) is mediated by changes in cellular redox homeostasis, which, through modulation of cell-signaling cascades, lead to a profound cytokinetic effect that engenders cell growth inhibition.

The cell lines used in this study originate from human colon, pancreatic, liver, breast and lung cancers and thus represent the major human cancers, which in 2006 accounted for ∼54% of all new cases of cancer in the USA. Among them, the most sensitive to P-ASA was HepG2 (IC_{50} = 13.8 μM), whereas the least sensitive was the pancreatic cell line MIA-PaCa2 (IC_{50} = 113 μM). Thus, it is clear that the tissue of origin of these carcinoma cell lines has limited influence on their responsiveness to P-ASA.

The results from the colon cancer cell lines, the largest group of cell lines from a single organ that we studied, revealed that P-ASA's effect was not significantly affected by individual variations in cell lines. Rather, their IC_{50}s fell within a relatively narrow range (14.3–67.6 μM), suggesting perhaps a broadly applicable mechanism of action.

An important finding was the uniform enhancement of the potency of P-ASA compared with conventional aspirin, whose precise IC_{50} could not be determined due to its limited solubility. In the 10 cell lines evaluated, the fold enhancement of potency ranged between >18 and >144, being on average >66.8. The reasons for the enhanced potency of P-ASA are not readily apparent, although they are clearly associated with the modification of aspirin's structure.

The growth inhibitory effect of P-ASA is brought about by a triple cell kinetic effect consisting of inhibition of proliferation, induction of apoptosis and necrosis, as well as the induction of cell cycle block at the G_2/M phase. Specifically, P-ASA inhibited cell proliferation concentration-dependently (this inhibition reached 68% at 50 μM P-ASA) and induced both early and late apoptosis as well as pure necrosis. Treatment with P-ASA 25 μM increased the amount of apoptotic cells 5.5-fold and of necrotic cells 4-fold, compared with controls. The greatest increase concerned late apoptosis. The relative contribution of each effect to the overall growth inhibitory effect of P-ASA cannot be quantified precisely, but it appears that the induction of apoptosis is the dominant cytokinetic effect.

As we have previously suggested, the induction of ROS by a chemopreventive agent is a mechanistic event that is both significant and

early (12,21). This proved to be the case for P-ASA as well. As our data clearly demonstrate, P-ASA enhanced the intracellular levels of ROS assayed using a 'general ROS probe', which reacts with several individual species. Although ROS measured by this probe increased by 36.5% in response to P-ASA, the main redox effect of P-ASA was on the levels of superoxide anion in mitochondria. Superoxide anions detected in the entire cell by DHE did not change in response to P-ASA, and NO levels, which might have contributed to the DCFDA response, were also unchanged. The most significant ROS increase (112% over control) concerned the mitochondrial superoxide anion, indicating that mitochondria are the most important target of P-ASA. Indeed, mitochondrial superoxide anion plays a critical role in the initiation of apoptotic cell death and this is what we observed in response to P-ASA.

The intrinsic (mitochondrial) pathway of apoptosis is characterized by cytochrome *c* release and activation of caspase 9 but not of caspase 8 (17). This form of apoptosis can be triggered by increased ROS, which permeabilize the mitochondrial membrane and release proapoptotic factors from the mitochondrial intermembrane space into the cytosol (22). Our data demonstrated that P-ASA activated caspase 9, while leaving caspase 8 intact. P-ASA increased mitochondrial ROS and led to the collapse of the mitochondrial membrane potential. Collectively, these findings establish that P-ASA targets the mitochondria and that this effect triggers the intrinsic apoptotic pathway. Further support that ROS are involved in the induction of cell death by P-ASA comes from the finding that the antioxidant agent NAC, which raises intracellular GSH levels, blocked both the rise of superoxide anion levels in the mitochondria and the induction of cell death by P-ASA.

The ROS levels in a cell represent the balance between ROS production and ROS inactivation by an intricate system of antioxidant mechanisms (23). GSH, one of the most important antioxidant mechanisms in mammalian cells, responds directly to intracellular redox changes and is also used as a cofactor for antioxidant enzymes (15). P-ASA depleted GSH stores in a concentration-dependent manner. That P-ASA may have increased ROS levels, at least in part, through its effect on GSH is evidenced by two manipulations of the system designed to affect the levels of GSH. First, BSO, which decreased intracellular GSH, reduced the IC_{50} of P-ASA for cell growth by more than half and second, supplementing the cells with NAC greatly attenuated the apoptotic effect of P-ASA. These effects are similar to those we obtained with nitroaspirin, a structurally similar compound, which depletes GSH by forming a conjugate with it (24).

The increase in intracellular levels of ROS by P-ASA had important repercussions for the fate of the cancer cell. Our findings make it clear that ROS, elevated in response to P-ASA, modulated predominantly three signaling pathways: MAPK, COX-2 and NF-κB. MAPKs, a family of serine/threonine kinases, play an essential role in signal transduction by modulating gene transcription in the nucleus in response to changes in the cellular environment (25). MAPKs are required for specialized cell functions controlling cell proliferation, cell differentiation, as well as cell death and are deregulated in several malignancies including colon cancer (26–28). We observed that P-ASA activated (by phosphorylation) p38 and JNK, while its effect on ERK1/2 was insignificant. It is noteworthy that the p38 and JNK 'branches' of the MAPK cascade are redox sensitive, whereas ERK, the one that remained unchanged, is not redox responsive (29). AKT, which inhibits apoptosis and is frequently altered in various human malignancies (30), was activated by P-ASA, albeit quite modestly. Interestingly, recent data suggest that antineoplastic compounds modulate this pathway and such effects may mediate their pharmacological activity (31). This seems to also be the case for P-ASA. Indeed, P-ASA could exert part of its pharmacological effect through modulation of MAPKs. This is supported by our previous observations that nitroaspirin, a structurally related compound, modulated MAPKs and the cell growth inhibitory effect of nitroaspirin was prevented by MAPK inhibitors and by silencing the p38 and JNK MAPKs (27).

Two signaling pathways that probably interact closely are COX and NF-κB, both regulate cell death and are of great importance to carcinogenesis (10). In particular, NF-κB, a mediator of inflammatory responses, is now emerging as a link between inflammation and cancer (32,33). P-ASA stimulated the expression of COX-2 and inhibited NF-κB signaling; the effect of P-ASA on both was redox dependent, as NAC reversed it. Although it is usually assumed that NF-κB activation induces COX-2, several other signaling cascades converge onto the *cox-2* promoter, including Sp-1, c-MYB, activator protein-1, T-cell factor, cAMP responsive element and activator protein-2 (34). Moreover, de Moraes *et al.* (34) suggest two different scenarios to explain COX-2 regulation. In the 'inflammatory scenario', p53 activated by DNA damage, recruits NF-κB to activate COX-2, resulting in antiapoptotic effects that contribute to cell expansion in inflammatory precursor lesions. However, in a 'constitutive proliferation scenario', oncogenic stress due to activation of growth signaling cascades (e.g. those involving Wnt/β-catenin, K-ras or c-Myb) upregulates *cox-2* independent of NF-κB to promote cancer progression (34). In agreement with the above, we have recently shown that several chemopreventive agents increase ROS production leading to COX-2 overexpression (35) and NF-κB inhibition (36). These chemopreventive agents, including P-ASA, affect the thioredoxin system that is essential to maintain critical cysteine residues of the p50 and p65 subunits in their reduced form, which is required for NF-κB binding to its consensus sequence (36). Thus, we postulate that P-ASA can activate COX-2, while inhibiting NF-κB binding.

Changes in cell signaling in response to pharmacological agents can be both extensive and complex. As we and others have pointed out (4), it is often difficult to discern the relevance to the final pharmacological result of each pathway that has been changed. This appears to be the case with our data. Nevertheless, it is conceivable that one or more of the effects of P-ASA on these signaling pathways could be pivotal for its remarkable pharmacological action.

In conclusion, our data demonstrate that P-ASA (MDC-43), which targets several types of cancer, possesses broad anticancer properties. P-ASA is significantly more potent than conventional aspirin in inhibiting cancer cell growth. Underlying this growth inhibition appears to be changes in cellular redox homeostasis, which activate significant intracellular signaling pathways probably culminating in a major cytokinetic effect. These findings make it clear that P-ASA is a promising novel agent for the control of cancer that merits further evaluation.

Funding

National Institutes of Health (2R01 CA92423, R01 CA101019).

Acknowledgements

Conflict of Interest Statement: None declared.

References

1. Baron,J.A. (2003) Epidemiology of non-steroidal anti-inflammatory drugs and cancer. *Prog. Exp. Tumor Res.*, **37**, 1–24.
2. Baron,J.A. *et al*. (2003) A randomized trial of aspirin to prevent colorectal adenomas. *N. Engl. J. Med.*, **348**, 891–899.
3. Rayyan,Y. *et al*. (2002) The role of NSAIDs in the prevention of colon cancer. *Cancer Invest.*, **20**, 1002–1011.
4. Rigas,B. (2007) The use of nitric oxide-donating nonsteroidal anti-inflammatory drugs in the chemoprevention of colorectal neoplasia. *Curr. Opin. Gastroenterol.*, **23**, 55–59.
5. Lazzarato,L. *et al*. (2008) Searching for new NO-donor aspirin-like molecules: a new class of nitrooxy-acyl derivatives of salicylic acid. *J. Med. Chem.*, **51**, 1894–1903.
6. Rigas,B. *et al*. (2008) The novel phenylester anticancer compounds: study of a derivative of aspirin (phoshoaspirin). *Int. J. Oncol.*, **32**, 97–100.
7. Kashfi,K. *et al*. (2005) Positional isomerism markedly affects the growth inhibition of colon cancer cells by nitric oxide-donating aspirin *in vitro* and *in vivo*. *J. Pharmacol. Exp. Ther.*, **312**, 978–988.
8. Tietze,F. (1969) Enzymic method for quantitative determination of nanogram amounts of total and oxidized glutathione: applications to mammalian blood and other tissues. *Anal. Biochem.*, **27**, 502–522.

9. Mackenzie,G.G. *et al*. (2004) Epicatechin, catechin, and dimeric procyanidins inhibit PMA-induced NF-kappaB activation at multiple steps in Jurkat T cells. *FASEB J.*, **18**, 167–169.
10. Williams,J.L. *et al*. (2008) NO-donating aspirin inhibits the activation of NF-kappaB in human cancer cell lines and Min mice. *Carcinogenesis*, **29**, 390–397.
11. Williams,J.L. *et al*. (2001) Nitric oxide-releasing nonsteroidal anti-inflammatory drugs (NSAIDs) alter the kinetics of human colon cancer cell lines more effectively than traditional NSAIDs: implications for colon cancer chemoprevention. *Cancer Res.*, **61**, 3285–3289.
12. Rigas,B. *et al*. (2008) Induction of oxidative stress as a mechanism of action of chemopreventive agents against cancer. *Br. J. Cancer*, **98**, 1157–1160.
13. LeBel,C.P. *et al*. (1992) Evaluation of the probe 2′,7′-dichlorofluorescin as an indicator of reactive oxygen species formation and oxidative stress. *Chem. Res. Toxicol.*, **5**, 227–231.
14. Meister,A. (1991) Glutathione deficiency produced by inhibition of its synthesis, and its reversal; applications in research and therapy. *Pharmacol. Ther.*, **51**, 155–194.
15. Klaunig,J.E. *et al*. (2004) The role of oxidative stress in carcinogenesis. *Annu. Rev. Pharmacol. Toxicol.*, **44**, 239–267.
16. Griffith,O.W. *et al*. (1979) Potent and specific inhibition of glutathione synthesis by buthionine sulfoximine (S-n-butyl homocysteine sulfoximine). *J. Biol. Chem.*, **254**, 7558–7560.
17. Watson,A.J. (2004) Apoptosis and colorectal cancer. *Gut*, **53**, 1701–1709.
18. Burgunder,J.M. *et al*. (1989) Effect of N-acetylcysteine on plasma cysteine and glutathione following paracetamol administration. *Eur. J. Clin. Pharmacol.*, **36**, 127–131.
19. Pathak,S.K. *et al*. (2005) Oxidative stress and cyclooxygenase activity in prostate carcinogenesis: targets for chemopreventive strategies. *Eur. J. Cancer*, **41**, 61–70.
20. Bubici,C. *et al*. (2006) The NF-kappaB-mediated control of ROS and JNK signaling. *Histol. Histopathol.*, **21**, 69–80.
21. Zhou,H. *et al*. (2009) Nitric oxide-donating aspirin inhibits the growth of pancreatic cancer cells through redox-dependent signaling. *Cancer Lett.*, **273**, 292–299.
22. Mukhopadhyay,P. *et al*. (2007) Simultaneous detection of apoptosis and mitochondrial superoxide production in live cells by flow cytometry and confocal microscopy. *Nat. Protoc.*, **2**, 2295–2301.
23. Halliwell,B. (2007) Oxidative stress and cancer: have we moved forward? *Biochem. J.*, **401**, 1–11.
24. Gao,J. *et al*. (2005) Nitric oxide-donating aspirin induces apoptosis in human colon cancer cells through induction of oxidative stress. *Proc. Natl Acad. Sci. USA*, **102**, 17207–17212.
25. Turjanski,A.G. *et al*. (2007) MAP kinases and the control of nuclear events. *Oncogene*, **26**, 3240–3253.
26. Chang,L. *et al*. (2001) Mammalian MAP kinase signalling cascades. *Nature*, **410**, 37–40.
27. Hundley,T.R. *et al*. (2006) Nitric oxide-donating aspirin inhibits colon cancer cell growth via mitogen-activated protein kinase activation. *J. Pharmacol. Exp. Ther.*, **316**, 25–34.
28. Manning,A.M. *et al*. (2003) Targeting JNK for therapeutic benefit: from junk to gold? *Nat. Rev. Drug Discov.*, **2**, 554–565.
29. Pearson,G. *et al*. (2001) Mitogen-activated protein (MAP) kinase pathways: regulation and physiological functions. *Endocr. Rev.*, **22**, 153–183.
30. Michl,P. *et al*. (2005) Mechanisms of disease: PI3K/AKT signaling in gastrointestinal cancers. *Z. Gastroenterol.*, **43**, 1133–1139.
31. Bode,A.M. *et al*. (2004) Targeting signal transduction pathways by chemopreventive agents. *Mutat. Res.*, **555**, 33–51.
32. Karin,M. *et al*. (2005) NF-kappaB: linking inflammation and immunity to cancer development and progression. *Nat. Rev. Immunol.*, **5**, 749–759.
33. Zhang,Z. *et al*. (2006) NF-kappaB, inflammation and pancreatic carcinogenesis: NF-kappaB as a chemoprevention target (review). *Int. J. Oncol.*, **29**, 185–192.
34. de Moraes,E. *et al*. (2007) Cross-talks between cyclooxygenase-2 and tumor suppressor protein p53: balancing life and death during inflammatory stress and carcinogenesis. *Int. J. Cancer*, **121**, 929–937.
35. Sun,Y. *et al*. (2008) Chemopreventive agents induce oxidative stress in cancer cells leading to COX-2 overexpression and COX-2-independent cell death. *Carcinogenesis,* in press.
36. Sun,Y. *et al*. (2008) The thioredoxin system mediates redox-induced cell death in human colon cancer cells: implications for the mechanism of action of anticancer agents. *Cancer Res.*, **68**, 8269–8277.

Received September 22, 2008; revised December 31, 2008; accepted January 5, 2009